Passively mode-locked diode-pumped solid-state lasers that use an antiresonant Fabry–Perot saturable absorber

K. J. Weingarten

Lightwave Electronics Corporation, 1161 San Antonio Road, Mountain View, California 94043

U. Keller, T. H. Chiu, and J. F. Ferguson

AT&T Bell Laboratories, Crawfords Corner Road, Holmdel, New Jersey 07733

Received November 19, 1992

We report passively mode-locked diode-pumped Nd:YAG and Nd:YLF lasers that use an antiresonant Fabry–Perot saturable absorber. For Nd:YLF at 1047 nm, we achieved pulses of 5.1 ps FWHM with 225 mW of average power. For Nd:YAG at 1064 nm, we achieved pulse widths of 8.7 ps with 100 mW of average power. Both lasers ran at a repetition rate of 100 MHz. The frequency stability of the free-running lasers was sufficient to allow locking of the laser repetition rate to a synthesizer by using a phase-lock-loop feedback system.

The study of passive mode locking of solid-state lasers has seen an incredible burst of activity over the past several years. In 1988, Blow and Woods theoretically predicted that any nonlinear coupled cavity would lead to passive mode locking.[1] This has led to many experimental demonstrations[2] of coupled-cavity mode locking such as additive-pulse mode locking[3,4] and resonant passive mode locking,[5,6] which have successfully mode locked Ti:sapphire, color-center, Nd:YLF, and Nd:YAG lasers. However, an intracavity mode-locking technique that would lead to a simpler cavity design and would not require active stabilization would be more desirable. Kerr lens mode locking[7–10] (KLM) is the simplest mode-locking technique but is not self-starting. Active mode locking typically requires a precisely fabricated transducer,[11] ≈1 W of rf drive power, and active stabilization of the cavity length to the drive frequency to maintain the shortest possible pulses.[12] The monolithic version of resonant passive mode locking is the antiresonant Fabry–Perot saturable absorber[13] (A-FPSA), which eliminates the coupled cavity and the need for active stabilization, dramatically increasing the robustness and utility of this technique. The A-FPSA has been demonstrated with Nd:YLF and Nd:YAG lasers end pumped with a Ti:sapphire laser. Here we extend this technique to diode-pumped Nd:YAG and Nd:YLF lasers and demonstrate phase locking of the free-running passive laser to an electronic synthesizer using a phase-lock loop.

Extension of this technique to diode pumping is not trivial. In general, solid-state laser materials typically have small gain cross sections ($\leq 10^{-19}$ cm^2), which requires a low-loss fast saturable absorber. A semiconductor saturable absorber directly inserted into a laser with these materials typically would have too much loss and too low a saturation intensity. Operating a Fabry–Perot absorber at antiresonance with a high reflectivity of the top mirror decreases the intensity inside the Fabry–Perot cavity with respect to the incident intensity. This transforms the saturable absorber to a high-saturation-intensity, low-loss device as required. Also, the unsaturated laser gain is significantly lower when it is diode pumped compared with that when it is pumped by a Ti:sapphire laser. This is due to several effects. First, the diode laser has a broader linewidth, which results in a longer average absorption length. Second, the diode laser has a spatial output that is many times diffraction limited and that cannot be focused to a near-diffraction-limited spot as the Ti:sapphire laser can, thus it requires a larger laser mode size to ensure mode matching, which reduces the laser's gain. The lower gain resulting from diode pumping requires more careful attention to the carrier lifetime and the effective absorber cross section (which is set by the top reflector R_1 of the A-FPSA in Fig. 1). Two conditions must be met: sufficiently nonlinearity must be available to start the laser, and the cavity losses need to be kept low to prevent Q switching so as to maintain low amplitude noise. These points are discussed in more detail below.

Figure 2 shows a schematic of the laser. The cavity[12,14] is similar to that used for active mode

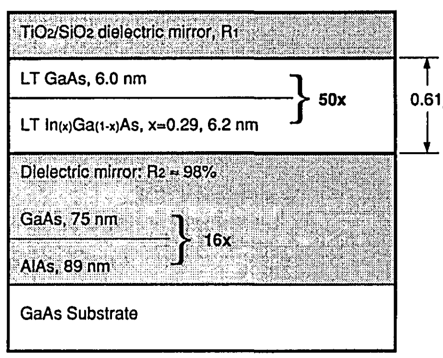

Fig. 1. Cross section of the A-FPSA device (not to scale). LT, low temperature.

0146-9592/93/080640-03$5.00/0

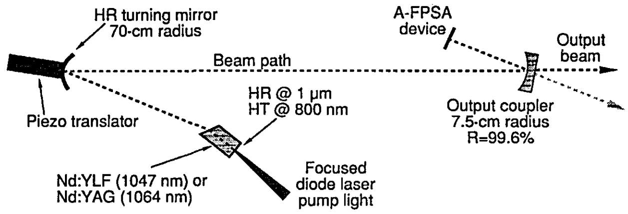

Fig. 2. Schematic of the laser cavity (not to scale). HT, highly transmitting.

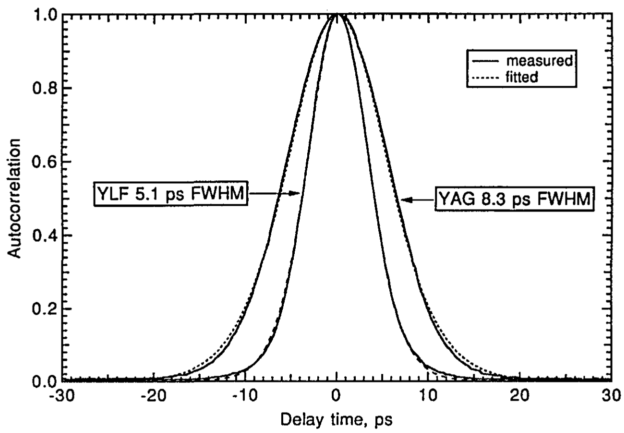

Fig. 3. Autocorrelation of passively mode-locked Nd:YLF and Nd:YAG lasers. The FWHM pulse width is determined from a best fit of an ideal sech^2 autocorrelation function.

locking, but the flat output coupler has been replaced with a curved mirror that focuses the light onto the saturable absorber.[13] The overall cavity length was approximately 1.5 m, which gives a nominal repetition rate of 100 MHz. The laser mode radius at the crystal flat is calculated to be 170 μm × 250 μm for YLF (170 μm × 310 μm for YAG), and at the A-FPSA it is calculated to be a 35-μm-radius circle. The 70-cm highly reflective (HR) turning mirror was 48 cm from the laser crystal. The A-FPSA device was 3.75 cm from the 7.5-cm $R = 99.6\%$ output coupler. The cavity has two output beams of roughly equal power; the output powers reported here were measured using only the beam traveling from the HR turning mirror through the output coupler. Other cavities are possible to eliminate this spurious output beam, which should double the available output power. For the Nd:YLF laser we used a 2-W diode (Spectra Diode Laboratories SDL 2372-P1) with an emitting aperture of 1 μm × 200 μm, and for the Nd:YAG laser we used a 1-W diode (Sony 304XT) with a similar 1 μm × 200 μm aperture size.

For Nd:YLF, we achieved pulses of 5.1 ps and 260-mW average power with a 35-ps carrier lifetime and 99% R_1 (Fig. 3). Using samples with shorter lifetimes and 99% R_1 resulted in insufficient nonlinearity for self-starting, and using samples with a 98% R_1 resulted in Q-switched mode-locked behavior. With Nd:YAG, the best results of 8.7 ps and 100 mW were achieved with a 35-ps lifetime and 98% R_1. Decreasing the coupling to $R_1 = 99\%$ resulted in insufficient nonlinearity for self-starting in Nd:YAG. Other lifetimes below 35 ps also resulted in stable mode locking when R_1 was 98%. Nd:YAG has an increased gain cross section and lower upper-state lifetime compared with those of Nd:YLF, which results in a reduced mode-locking buildup time and an improved threshold for self-Q-switching (see the discussion below). The laser's optical spectrum was not measured when it was diode pumped; however, we expect it to be similar to the spectrum measured when it was end pumped with a Ti:sapphire laser, which typically had a spectrum 1.6 to 1.9 times the ideal time–bandwidth product for a sech^2 pulse.

Self-starting is an important issue for passive mode locking. The A-FPSA's change in absorption owing to carrier recombination on the picosecond time scale provides the starting mechanism[15] that nonresonant techniques such as KLM lack. This means that these lasers run mode locked continuously without intermittent dropouts and without requiring a mechanical perturbation to restart the laser.

Another important issue when using an A-FPSA with lasers that have long upper-state lifetimes is self-Q-switching.[15] When the laser is running self-Q-switched, the autocorrelation typically appears stable, similar to that under normal, non-Q-switched operation. We check for self-Q-switching by looking at the relaxation oscillation sidebands of the laser intensity using a microwave spectrum analyzer. When the laser is running with stable mode-locked pulses, the relaxation oscillation sidebands are

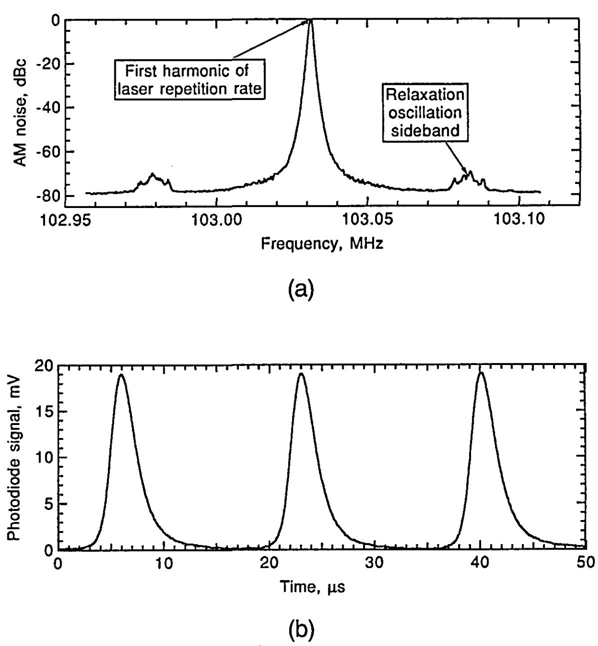

Fig. 4. (a) Typical amplitude noise spectrum when the laser is operating without self-Q-switching, measured around the first laser harmonic at 100 MHz on an rf spectrum analyzer with 1-kHz resolution bandwidth. (b) The pulse train envelope showing strong self-Q-switching behavior as observed in the time domain with a photodetector and oscilloscope. The autocorrelation during this operation has stability comparable with that of clean cw mode-locked operation. The corresponding spectrum would have sidebands approaching the level of the first harmonic in (a).

typically −60 dBc or less, as indicated in Fig. 4(a). This corresponds to an integrated amplitude noise of less than 1% rms. Self-Q-switching would result in relaxation oscillations sidebands approaching the level of the harmonic signal in the frequency domain. Figure 4(b) shows the corresponding time-domain signal under strong self-Q-switching. The pulse train envelope has microsecond-long macropulses that are separated by an interval approximately equal to the inverse of the small-signal relaxation oscillation frequency. Typically, we consider Q-switched operation deleterious; however, some applications may benefit from the higher peak power available when the laser operates in this mode.

Increasing the carrier lifetime (which can be controlled by the molecular-beam-epitaxy growth temperature) decreases the mode-locking buildup time (i.e., increases the mode-locking driving force).[15] However, increased carrier lifetime also increases the tendency to self-Q-switch, in effect because the longer lifetime provides lower-frequency modulation to the laser, which more strongly couples to the relaxation oscillations. Increasing the coupling into the device (i.e., decreasing R_1) also increases the driving force but increases the tendency to Q switch by increasing the cavity loss and the magnitude of the relaxation oscillations. Laser material parameters that decrease the magnitude of the relaxation oscillations and push them to higher frequency, such as lower upper-state lifetime of the laser material and higher gain cross section, result in a reduced threshold for self-Q-switching. This explains why Nd:YAG could be mode locked with a longer carrier lifetime sample, increased device coupling, and lower pump power compared with Nd:YLF. For the Nd:YAG laser with the 1-W diode-laser pump, we measured a typical relaxation oscillation frequency of 56.5 kHz and estimated the small-signal gain to be 30% (Ref. 15) (assuming an upper-state lifetime of $\tau = 230\ \mu s$), compared with a relaxation oscillation frequency of 60 kHz and a gain of 70% ($\tau = 480\ \mu s$) for the Nd:YLF laser when it was pumped with the 2-W diode laser.

With a free-running, passively mode-locked laser, the repetition rate is set by the inverse of the cavity round-trip time. For applications requiring synchronization to an external signal generator, the laser can be phase locked by controlling the cavity length. We have tested the feasibility of this approach by implementing a phase-lock-loop system in which the cavity length is controlled by placing one of the laser mirrors on a piezo transducer.[16] We demonstrated a stable, locked loop, verified by observing the repetition rate on a spectrum analyzer and by adjusting the cavity length with a manual translation stage and observing the corresponding change in the piezo transducer's servo voltage. For a phase detector with good AM noise rejection[17] and with appropriate piezo and loop response, we expect subpicosecond timing jitter using this approach.

In conclusion, we have demonstrated diode-pumped, passively mode-locked lasers with many of the features necessary for practical applications, such as seeding of regenerative amplifiers, optical probing of integrated circuits,[18] and medical and optoelectronic applications.[19] These lasers are simple and robust with clean spatial, temporal, and near-transform-limited spectral properties. Adjustment of the A-FPSA carrier lifetime and coupling was necessary to optimize the self-starting performance for both diode-pumped Nd:YLF and Nd:YAG lasers. In general, the absorption edge of the A-FPSA can be varied by adjusting the semiconductor's band-gap energy, which will allow extension of this technique to other diode-pumped laser materials and wavelengths.

The authors thank F. Adams of Lightwave Electronics Corporation for his assistance with the phase-lock-loop system. Lightwave Electronics Corporation acknowledges the partial support of this research by the U.S. Department of Energy under the Small Business Innovative Research Program.

References

1. K. J. Blow and D. Wood, J. Opt. Soc. Am. B **5**, 629 (1988).
2. For a review of recent research see the special issue on ultrafast optics and electronics in IEEE J. Quantum Electron. **28**, 2086–2229 (1992).
3. K. J. Blow and B. P. Nelson, Opt. Lett. **13**, 1026 (1988).
4. P. N. Kean, X. Zhu, D. W. Crust, R. S. Grant, N. Landford, and W. Sibbett, Opt. Lett. **14**, 39 (1989).
5. U. Keller, W. H. Knox, and G. W. 'tHooft, IEEE J. Quantum Electron. **28**, 2123 (1992).
6. U. Keller, W. H. Knox, and H. Roskos, Opt. Lett. **15**, 1377 (1990).
7. D. E. Spence, P. N. Kean, and W. Sibbett, Opt. Lett. **16**, 42 (1991).
8. U. Keller, G. W. 'tHooft, W. H. Knox, and J. E. Cunningham, Opt. Lett. **16**, 1022 (1991).
9. G. P. A. Malcolm and A. I. Ferguson, Opt. Lett. **16**, 1987 (1991).
10. K. X. Liu, C. J. Flood, D. R. Walker, and H. M. van Driel, Opt. Lett. **17**, 1361 (1992).
11. U. Keller, K. J. Weingarten, K. D. Li, D. C. Gerstenberger, P. T. Khuri-Yakub, and D. M. Bloom, Opt. Lett. **15**, 45 (1990).
12. K. J. Weingarten, M. Gifford, and L. Generali, in *Digest of Conference on Lasers and Electro-Optics* (Optical Society of America, Washington, D.C., 1991), paper CTHR15.
13. U. Keller, D. A. B. Miller, G. D. Boyd, T. H. Chiu, J. F. Ferguson, and M. T. Asom, Opt. Lett. **17**, 505 (1992).
14. D. C. Hanna, IEEE J. Quantum Electron. **QE-5**, 483 (1969).
15. U. Keller, T. H. Chiu, and J. F. Ferguson, Opt. Lett. **18**, 217 (1993).
16. S. B. Darack, D. R. Dykaar, and G. T. Harvey, Opt. Lett. **16**, 1677 (1991).
17. M. J. W. Rodwell, D. M. Bloom, and K. J. Weingarten, IEEE J. Quantum Electron. **25**, 817 (1989).
18. K. J. Weingarten, M. J. W. Rodwell, and D. M. Bloom, IEEE J. Quantum Electron. **24**, 198 (1988).
19. N. Streibl, K.-H. Brenner, A. Huang, J. Jahns, J. Jewell, A. W. Lohmann, D. A. B. Miller, M. Murdocca, M. E. Prise, and T. Sizer, Proc. IEEE **77**, 1954 (1989).